

Advances in Tropical Cyclone Intensity Forecasts

Robert Atlas¹
Vijay Tallapragada²
Sundararaman Gopalakrishnan¹

¹NOAA-Atlantic Oceanographic and Meteorological Laboratory/Hurricane Research Division
Miami, FL 33149

²NOAA-National Centers for Environmental Prediction/Environmental Modeling Center
College Park MD 20740

1 **Abstract**

2 NOAA established the 10 year Hurricane Forecast Improvement Project (HFIP) to
3 accelerate the improvement of forecasts and warnings of tropical cyclones and to enhance
4 mitigation and preparedness by increased confidence in those forecasts. Specific goals include
5 reducing track and intensity errors by 20% in 5 years and 50% in ten years and extending the
6 useful range of hurricane forecasts to 7 days. Under HFIP, there have been significant
7 improvements to NOAA's operational hurricane prediction model resulting in increased
8 accuracy in the numerical guidance for tropical cyclone intensity predictions. This paper
9 documents many of the improvements that have been accomplished over the last 5 years, as well
10 as some future research directions that are being pursued.

11 **Keywords:** Hurricane, Hurricane Forecast Improvement Program (HFIP), Hurricane
12 Weather Research and Forecasting Model (HWRF).

13

14 **1. Introduction**

15 Each year hurricanes, typhoons, and other tropical cyclones (TC) cause extensive
16 damage and loss of life throughout the world. Severe examples include the TC that
17 killed more than 300,000 people in Bangladesh in 1970; the Galveston, Texas hurricane of
18 1900, which destroyed the city and killed between 6000-8000 people; Hurricane Andrew
19 (1992), which caused monetary losses of 26.5 billion dollars; and Hurricane Katrina
20 (2005), which killed more than 1300 people and resulted in losses in excess of 100 billion
21 dollars. Even storms of much lesser intensity can produce significant loss of life and
22 property, presenting a daunting challenge for hurricane forecasters and the communities
23 they serve.

24 The reduction of losses related to hurricanes involves many complex aspects, ranging
25 from purely theoretical, observational, computational, and numerical, to operational and
26 decision-making. A correct warning can lead to an appropriately scaled and timed evacuation
27 and damage mitigation, producing immense benefits. However, over-warning can lead to
28 substantial unnecessary costs, a reduction of confidence in warnings, and a lack of
29 appropriate response. Therefore, accurate forecasts of hurricane track and intensity are of
30 great importance.

31 TC forecasting methods have evolved considerably. The earliest methods were primarily
32 subjective and were limited to forecasting the motion of TCs. Initially, these methods were based
33 on local observations of high level cloud and ocean swell movements, and later were based on
34 the application of steering patterns on synoptic charts. The past decades have been marked by
35 significant advances in dynamical models such as the National Oceanic and Atmospheric
36 Administration's (NOAA) Global Forecast System (GFS), the US Navy Operational Global

37 Atmospheric Prediction System (NOGAPS), the European Centre for Medium-Range Weather
38 Forecasts (ECMWF) model, and the Met Office model (UKMET). Such advances have
39 contributed greatly to a steady improvement in the official TC track forecasts issued by the
40 NOAA/National Weather Service's (NWS) National Hurricane Center (NHC), resulting in a
41 substantial reduction in track forecast errors (Gopalakrishnan et al., 2012). This, in turn, has
42 reduced warning and evacuation areas, thereby saving lives and resources (Rappaport et al.,
43 2009).

44 Forecasting intensity changes is also extremely important, especially in the case of storms
45 that rapidly intensify or weaken just prior to landfall (e.g., TCs Charley, 2004; Katrina and
46 Wilma, 2005; Humberto, 2007; Karl, 2010). However, forecasting intensity changes in TCs is a
47 complex and challenging multiscale problem. Since the 1950s, both statistical and dynamical
48 methods have been adopted to tackle this problem (Anthes, 1982). For instance, the Statistical
49 Hurricane Intensity Prediction Scheme (SHIPS) is a sophisticated statistical model that predicts
50 storm intensity using multiple regression relationships with climatological, persistence, and GFS
51 model predictors (DeMaria and Kaplan, 1999; DeMaria et al., 2005). DSHIPS (Decay-SHIPS) is
52 SHIPS adjusted for the decay of storms when they move inland, according to DeMaria et al.
53 (2006), and is regarded by the forecasters as one of the most reliable intensity forecast models
54 (Franklin, 2010).

55 During the past three years, significant progress has been made in TC track, intensity, and
56 structure forecasts with support from NOAA's Hurricane Forecast Improvement Project (HFIP,
57 Gall et al., 2013). In particular, for the first time, a very high-resolution (3 km) deterministic
58 numerical weather prediction (NWP) model, known as the Hurricane Weather Research and

59 Forecast (HWRF) modeling system, has shown comparable and, at times, superior TC intensity
60 forecast skill compared to the best performing statistical models.

61 HWRF was jointly developed by NOAA's Environmental Modeling Center (EMC) and
62 Hurricane Research Division (HRD) and implemented at the National Centers for Environmental
63 Prediction (NCEP). The HWRF model is now paving the way to improve operational TC
64 intensity forecasts, which have had virtually no improvement in skill for the last two decades.
65 This paper summarizes recent advances in hurricane modeling at NOAA, in collaboration with
66 academic and international partners, which has provided improved operational numerical
67 forecast guidance on TC track, intensity, and structure to the forecasters at NHC, the Central
68 Pacific Hurricane Center (CPHC), and the US Navy and Air Force Joint Typhoon Warning
69 Center (JTWC). Future development activities are also discussed.

70 **2. NOAA Hurricane Forecast Improvement Project**

71 Since its official start in 2010, HFIP has been providing a unified organizational
72 infrastructure and funding for NOAA and other agencies to coordinate the hurricane research
73 needed to significantly improve guidance for hurricane track, intensity, and storm surge
74 forecasts. HFIP's 5-year (for 2014) and 10-year (for 2019) goals are to:

- 75 • Reduce average track errors by 20% in 5 years; 50% in 10 years for days 1 through 5.
- 76 • Reduce average intensity errors by 20% in 5 years; 50% in 10 years for days 1 through 5.
- 77 • Increase the probability of detection for rapid intensification (RI) to 90% at day 1,
78 decreasing linearly to 60% at day 5, and decrease the false alarm ratio for RI change to
79 10% for day 1, increasing linearly to 30% at day 5.

- 80 • Extend the lead time for hurricane forecasts out to day 7 (with an accuracy equivalent to
81 that of the day 5 forecasts when they were introduced in 2003).

82 It is hypothesized that the HFIP goals could be met with high-resolution (~10-15 km)
83 global atmospheric numerical forecast models run as an ensemble in combination with, and as a
84 background for, regional models at even higher resolution (~1-5 km). HFIP expects that its
85 intensity goals will be achieved through the use of regional models with a horizontal resolution
86 near the core finer than about 3 km. This paper focuses on the intensity forecast improvements
87 obtained from the NCEP HWRF modeling system during the first phase (i.e., first 5 years) of
88 HFIP.

89 **3. NCEP HWRF Modeling System**

90 Specialized regional TC models used at NCEP, the Geophysical Fluid Dynamics
91 Laboratory (GFDL) hurricane model (Bender et al., 2007) and the HWRF model (Tallapragada
92 et al., 2014b), are designed to provide real-time TC forecasts to NHC for the North Atlantic
93 (NATL) and eastern North Pacific (EPAC) basins, to the CPHC for the Central Pacific (CPAC)
94 basin, and to the JTWC for all tropical ocean basins including the northwestern Pacific (WPAC),
95 North Indian Ocean (NIO), South Indian Ocean (SIO), and Southern Pacific (SP). The GFDL
96 model was one of the primary track and intensity prediction tools used by NHC forecasters after
97 it became operational in 1994. In addition, the US Navy version of the GFDL model (GFDN) has
98 been used by the JTWC since 2002. With an aim to replace the hydrostatic GFDL model with a
99 more advanced atmosphere-ocean coupled non-hydrostatic model with storm following nests
100 capable of producing high-resolution TC forecasts, the HWRF modeling system was developed

101 and implemented at NCEP in 2007. Figure 1 shows the regions where the HWRF and
102 GFDL/GFDN models are currently operational in real time.

103 **4. HWRF Forecast Improvements in the North Atlantic Basin**

104 In the early 2000s, the development of an operational TC forecast system with a non-
105 hydrostatic dynamic core was started at the NCEP-EMC to better forecast TC intensity,
106 structure, and rapid intensity changes. In fulfillment of this goal, the HWRF modeling system
107 was established in 2007 to provide NHC with improved operational track and intensity forecast
108 guidance. The original HWRF model operated at a resolution of 27 km for the static domain and
109 9 km for the single movable nest. Meanwhile, HRD scientists developed an experimental
110 research version of HWRF called HWRFx (Zhang et al., 2011) to target the intensity change
111 problem at a higher resolution (about 3 km, Gopalakrishnan et al., 2011, 2012). Central to the
112 development of the high resolution HWRF model is the improvement of the surface and
113 boundary layer parameterization schemes. Inner-core data collected by NOAA's WP-3D
114 research aircraft were used as the basis to redesign the parametrization schemes for high-
115 resolution hurricane applications (Gopalakrishnan et al., 2013). Significant improvements to the
116 model forecasted boundary layer structure, as well as size predictions, were demonstrated with
117 those advances. Supported by HFIP, a triply-nested, high-resolution HWRF system (27:9:3 km)
118 with improved physics that were calibrated to match observations was run in real-time
119 demonstration mode in 2011.

120 Based on HFIP demonstration experiments that illustrated significant impacts of high
121 resolution for TC predictions (Gopalakrishnan et al., 2012), scientists at EMC worked with
122 NOAA research partners, in particular at HRD and academic institutions, and implemented
123 major changes to the original operational version of HWRF, resulting in a new operational

124 HWRF model at NCEP for the 2012 hurricane season (Tallapragada et al., 2013; Goldenberg et
125 al., 2015). The central improvement was the triple-nest capability (27:9:3 km) that included a
126 cloud-resolving innermost grid operating at 3 km horizontal resolution, along with several
127 improvements to the physics schemes based on observational findings and advanced vortex
128 initialization data assimilation techniques for better representation of the inner core structure of
129 storms. Apart from obtaining significant improvements in track forecast skill compared to
130 previous versions, the 2012 version of the operational HWRF model conclusively demonstrated
131 the positive impact of resolution on storm size and structure forecasts (Tallapragada et al., 2013).

132 The 2013 version of the operational HWRF model made significant additional
133 improvements in track, intensity, and structural prediction of TCs by taking better advantage of
134 the high-resolution capability built into the 2012 HWRF model (Bernardet et al., 2015). For the
135 first time, the HWRF Data Assimilation System (HDAS), a Gridpoint Statistical Interpolation
136 (GSI) based one-way hybrid ensemble-variational data assimilation scheme, was implemented to
137 assimilate inner-core observations from the NOAA WP-3D aircraft Tail Doppler Radar (TDR)
138 data in real-time, when available. One of the highlights of the 2013 HWRF configuration
139 retrospective tests and evaluations performed on a sample of named TCs, comprised of 835 cases
140 from three North Atlantic hurricane seasons (2010-2012), was the remarkable reduction of
141 intensity forecast errors. Results shown in Figure 2 indicate that the 2013 HWRF model
142 (denoted by H3FI) outperformed the statistical models (DSHP: Decay SHIPS and LGEM: Linear
143 Growth Equation Model), operational HWRF (HWFI), operational GFDL (GHMI), and 2012
144 version of HWRF (H2FI), as well as the NHC Official (OFCL) forecasts for intensity prediction
145 in the 2-3 day forecast period. Historically, statistical models have been more skillful than
146 dynamical models for hurricane intensity prediction.

147 Upgrades to the HWRF system continue on an annual basis. Each new configuration of
148 the HWRF model is implemented for operations at the start of hurricane season for NHC
149 forecasters to have access to improved hurricane guidance. Systematic evaluation of each
150 individual upgrade (and combinations thereof) for multiple hurricane seasons is the key element
151 of model development activities at NCEP supported by HFIP, and this process ensures
152 appropriate testing of model stability, reliability, and expected performance levels in real-time
153 operations. Important upgrades to the 2014 version of the operational HWRF model (H214)
154 include increased vertical resolution (61 levels), a higher model top (2 hPa), assimilation of
155 aircraft reconnaissance dropsonde data in the inner core, and implementation of a new, high-
156 resolution version of the POM-TC (MPIPOM-TC) ocean model. An evaluation of the 2014
157 HWRF upgrades has shown further improvements in track and intensity forecasts, with the
158 average track errors now comparable to the GFS model and average absolute intensity errors
159 better than NHC's official forecasts at all forecast times. Figure 3 shows the cumulative
160 improvements obtained from the operational HWRF model during the last 4 years (2011-2014),
161 highlighting the role of HWRF in providing more accurate track and intensity forecast guidance
162 for NHC.

163 ***4.1 Experimental Real-Time HWRF Forecasts for the WPAC Basin in Support of JTWC***

164 The progress in the NATL basin prompted the HWRF team at EMC to provide
165 experimental real-time guidance to JTWC for typhoon forecasts in the WPAC basin starting in
166 2012, using the same operational HWRF model implemented at NCEP, except for the ocean
167 coupling (i.e., sea surface temperatures did not evolve during the forecasts over the WPAC
168 basin). An evaluation of model performance in 2012 showed lower forecast track and intensity
169 errors for the HWRF model compared to other operational regional models then used by JTWC

170 (Evans and Falvey, 2013; Tallapragada et al., 2015a). Intensity forecasts also showed improved
171 performance as compared to other regional models with much reduced forecast errors during the
172 first 24 h owing to better vortex initialization. These experimental forecasts were performed with
173 computational resources and support provided by HFIP and delivered to JTWC with about 85%
174 real-time reliability achieved through specially-established procedures. Given the positive
175 performance of the HWRF model in the WPAC basin during the 2012 season, the HWRF team
176 at EMC continued its efforts to provide real-time forecasts in 2013 and 2014 using the 2013
177 upgrade of the HWRF model.

178 Performance of the HWRF model during the real-time experiments in the 2012-2013
179 typhoon seasons is shown in Figure 4. Non-homogeneous seasonal statistics of the absolute TC
180 track forecast errors and the absolute intensity errors in the WPAC basin between the 2012-2013
181 seasons are provided in this figure (Tallapragada et al., 2015a, 2015b). One notices a very
182 significant improvement of the 2013 HWRF model compared to the 2012 version of HWRF with
183 both the track and intensity forecast errors reduced at all forecast lead times.

184 Given the fact that the WPAC basin was very active in 2013 with 34 storms, of which
185 five were super typhoons (STY) including the extremely powerful landfalling STY Haiyan, the
186 improvement seen in the intensity and track forecast errors at the 3-5 day lead times is strong
187 evidence that HWRF improves the forecasts of structure and development of TCs in the WPAC
188 basin. The performance and reliability of the HWRF forecasts allowed JTWC to officially
189 include HWRF as one of their track and intensity consensus models. Figure 5 shows the
190 homogeneous verification of HWRF relative to the suite of other operational models used by
191 JTWC, namely COAMPS-TC (Naval Research Laboratory Coupled Ocean-Atmosphere
192 Prediction System for TCs, referred to as COTC), GFDL, GFDN, NCEP GFS, and the official

193 JTWC forecasts for WPAC typhoons in 2013. HWRF outperformed all other regional models in
194 terms of track and intensity forecasts, with HWRF's track errors comparable to the global GFS
195 forecasts except at day 4, and HWRF's absolute intensity errors demonstrated consistently better
196 forecasts than all other models during the entire 5-day forecast times.

197 **4.2 Evolution of HWRF as a Unique, High Resolution Regional Hurricane Model with** 198 **Extended Coverage over Indian Seas**

199 The successful demonstration of the HWRF model's performance for the WPAC basin
200 led to expanding the scope of the real-time experimental forecasts from HWRF to all world
201 tropical oceanic basins. HWRF forecast guidance for track, intensity, structure, and rainfall for
202 all six tropical cyclones that formed in the NIO basin during 2013 were provided to the India
203 Meteorological Department (IMD) Cyclone Warning Division (CWD), including the very severe
204 cyclone Phailin. IMD has been routinely using the operational forecast guidance from the NCEP
205 models and acknowledged the superior quality of the products they received from NCEP
206 (Mohapatra, personal communication). An example illustrating the HWRF model's forecasts for
207 the life cycle, from genesis to landfall, of TC Phailin is shown in Figure 6. The improved
208 numerical model forecast guidance for the track, intensity, structure, and storm surge 4-5 days
209 prior to the landfall of TC Phailin, and the enhanced warning products that were disseminated
210 collectively, helped disaster management personnel evacuate more than a million people in India
211 from potentially affected areas to cyclone shelters, safe houses, and inland locations (Mohanty et
212 al., 2015).

213 Track and intensity forecast error statistics (Figure 7) for all six tropical cyclones that
214 formed in the NIO basin during 2013 indicated the superior performance of the HWRF model at
215 almost all forecast times compared to other model guidance received by JTWC.

216 **4.3 Rapid Intensification and Intensity Change Forecasts from HWRF: A Major**
217 **Accomplishment**

218 Improving RI¹ forecasts is one of the highest priorities for TC forecasters at NHC and
219 JTWC and has been recognized as the most challenging aspect of TC research. Much of the lack
220 of improvement in the RI forecast skill is rooted in our lack of understanding on when and how
221 RI occurs in different environmental conditions and the historic inability of dynamical models to
222 adequately predict the multi-scale processes that produce an RI event. The impressive intensity
223 forecast performance from the new operational HWRF model has demonstrated its improved
224 ability in representing and forecasting RI, as shown through extensive numerical experiments
225 and observations for Hurricane Earl (2010), a hurricane that intensified even when the
226 environmental vertical wind shear was very large (Chen and Gopalakrishnan, 2015).

227 In that study, Chen and Gopalakrishnan performed a simulation of Hurricane Earl (2010)
228 using the operational 2013 HWRF system, verified the predictions against available inner-core
229 observations, and used the simulation to understand the asymmetric RI of a TC in a sheared
230 environment. The forecast verification illustrated that the HWRF model realistically simulated
231 Hurricane Earl's observed evolution of intensity, as well as several aspects of its inner-core
232 structure, including convective and wind asymmetries and vortex tilt² prior to and during RI. An
233 examination of the high-resolution forecast data revealed that Hurricane Earl's tilt was large at
234 the RI onset and decreased quickly once RI commenced, suggesting vertical alignment is the
235 result instead of the trigger for RI.

236 Furthermore, this study found that the RI onset is associated with the development of
237 upper-level warming in the eye region. A thermodynamic budget calculation showed that
238 warming over the low-level center results primarily from radially inward storm-relative

¹An increase in maximum sustained winds of a TC by at least 30 knots in a 24-h period.

²As measured by the circulation centers at 2- and 8-km altitude (Figure 5 in Chen and Gopalakrishnan, 2015).

239 advection of subsidence-induced warm air in the upshear-left region. This advection does not
240 occur until persistent convective bursts (CBs) are concentrated in the downshear-left quadrant. It
241 is the favorable juxtaposition of convective-scale subsidence and the broader-scale, shear-
242 induced subsidence which is most conducive for intensification. When CBs are concentrated in
243 the downshear-left and upshear-left quadrants, the net subsidence warming is maximized
244 upshear, and the resulting warm air is advected over the low-level storm center by the upper-
245 level, storm-relative flow. Subsequently, the surface pressure falls and RI occurs. This HWRP
246 simulation of Earl provides a promising baseline for understanding the RI problem in three
247 dimensions during a time period when the resolution of observations was not high enough to
248 study the evolution of RI and vortex tilt.

249 RI events appear more frequently in WPAC compared to other basins, thus allowing for
250 extensive examination of the capability of the HWRP model in forecasting these events. Using
251 an idealized configuration, Bao et al. (2012), Gopalakrishnan et al. (2011, 2013), and Kieu et al.
252 (2014) demonstrated that the onset of RI in the HWRP model only occurred when a specific set
253 of conditions were present in the modeled storm's dynamic and thermodynamic structure (i.e.,
254 phase-lock condition). Specifically, the HWRP model vortex must possess three basic
255 ingredients for RI onset to occur, namely: (1) a warm anomaly of 1-3 K around 400-300 hPa; (2)
256 a moist column with relative humidity >95% within the storm central region; and (3) low-level
257 tangential flow $\geq 15 \text{ m s}^{-1}$ (Figure 8a). Examples of the vertical structure of modeled storms right
258 at the onset of RI about 24 h into the forecast of STY Usagi initialized at 1800 UTC 16
259 September (Figure 8b) and for a forecast of STY Soulik that was initialized at 0600 UTC 7 July
260 (Figure 8c) show strikingly similar and coherent structure with all three components of the
261 phase-lock condition present at the RI onset (Tallapragada and Kieu, 2014a).

262 Verification of the probability of detection (POD) and the false alarm rate (FAR) of RI
263 forecasts for the WPAC basin during 2013, shown in Figure 9, indicates further improvements in
264 the POD for the 2013 HWRF model compared to the 2012 version. Specifically, the POD index
265 for RI forecasts (at >30 kt intensity change in 24 h) in the 2013 HWRF model is 0.22 compared
266 to 0.09 in 2012. While the POD index is still quite low, it is far better than other models used by
267 JTWC and their official forecasts (Tallapragada and Kieu, 2014a). A significant reduction in the
268 FAR index (from 0.81 in 2012 to 0.45 in 2013) also indicates improved reliability of RI forecasts
269 from the HWRF model in 2013.

270 **5. Future Directions for HWRF**

271 This work demonstrates the advances and steep-step performance improvements in the
272 operational the HWRF system. These significant improvements obtained with the new HWRF
273 implementation are attributed to a number of major changes since 2012, including a new, higher
274 resolution nest that is capable of better resolving eyewall convection and scale interactions,
275 improved vortex initialization, improved planetary boundary layer and turbulence physics, an
276 improved nest motion algorithm and, above all, systematic testing and evaluation (T&E) that are
277 not only based on single simulations and idealized case studies, but on several seasons of testing.
278 This kind of development and T&E would not be possible without the support of the HFIP high
279 performance computing capability.

280 Although the operational HWRF system is showing exceptional skill in intensity
281 forecasting, experience with TCs such as Irene (2011), Isaac (2012), and Sandy (2012) have
282 illustrated the importance of providing more accurate structure (e.g., size) and rainfall
283 predictions. The current operational HWRF configuration is storm centric and single nested, not
284 ideal for representing multi-scale interactions or for TC genesis forecast applications; it is greatly

285 limited in extending forecast lead times beyond 5 days. A key for improving TC forecasts of
286 genesis, size near landfall, rainfall post-landfall, and for extending forecast lead times beyond 5
287 days lies in the creation of a basin-scale model (eventually covering the entire globe) with
288 multiple moving nests at 1-3 km resolution covering all the storms in the basin. Based on the
289 2013 HWRF system that includes the operational initialization scheme and recent upgrades to
290 physics, HRD and NCEP-EMC researchers have created a basin scale HWRF system that can
291 operate with multiple moving nests at resolutions as high as 3 km now (Figure 10) and
292 potentially at higher resolution in the near future.

293 An additional area where significant improvement is needed is the initial conditions for
294 HWRF. To this end, improvements to data assimilation methodology and use of all available
295 hurricane observations are being pursued. This includes the development and deployment of new
296 observing systems (such as Doppler wind lidar) on NOAA's hurricane hunter aircraft and
297 conducting Observing System Simulation Experiments (OSSEs) to evaluate sampling strategies
298 for both reconnaissance aircraft and unmanned aerial systems, as well as to evaluate the potential
299 impact of new space-based observing systems (Atlas et al., 2015).

300 ***Acknowledgments.*** The authors acknowledge Drs. Frank Marks, Fred Toepfer, and Ed
301 Rappaport for their many important contributions to HFIP. We also thank the HWRF model
302 development teams at EMC and HRD for their outstanding contributions to improve the HWRF
303 model. Thanks are due to Ms. Gail Derr for offering editorial support.

304 **References**

- 305 Anthes, R.A. 1982. Tropical Cyclones: Their evolution, structure, and effects. Meteor. Monogr.
306 No. 41. Amer. Meteor. Soc. Boston, MA 208 pp.
- 307 Atlas, R., L. Bucci, B. Annane, R. Hoffman, A. Aksoy, S. Murillo, J. Delgado, S.J. Majumdar
308 and L. Cucurull. 2015. Observing System Simulation Experiments to assess the potential
309 impact of proposed observing systems on hurricane prediction. Mar. Tech. Soc. J. (in this
310 issue).
- 311 Bao, J.-W., S.G. Gopalakrishnan, S.A. Michelson, F.D. Marks Jr. and M.T. Montgomery. 2012.
312 Impact of physics representations in the HWRF on simulated hurricane structure and
313 pressure–wind relationships. Mon. Wea. Rev. 140:3278–99.
- 314 Bender, M., I. Ginis, R. Tuleya, B. Thomas and T. Marchok. 2007. The operational GFDL
315 Coupled Hurricane-Ocean Prediction system and a summary of its performance. Mon.
316 Wea. Rev. 135:3965-89.
- 317 Bernardet, L., V. Tallapragada, S. Bao, S. Trahan, Y. Kwon, Q. Liu, M. Tong, M. Biswas, T.
318 Brown, D. Stark, L. Carson, R. Yablonsky, E. Uhlhorn, S. Gopalakrishnan, X. Zhang, T.
319 Marchok, B. Kuo and R. Gall. 2015. Community support and transition of research to
320 operations for the Hurricane Weather Research and Forecasting model. Bull. Amer.
321 Meteor. Soc. 96(6):953-60.
- 322 Chen, H. and S.G. Gopalakrishnan. 2015. A study on the asymmetric rapid intensification of
323 Hurricane Earl (2010) using the HWRF System. J. Atmos. Sci. 72(2):531-50.
- 324 DeMaria, M. and J. Kaplan. 1999. An updated Statistical Hurricane Intensity Prediction Scheme
325 for the Atlantic and eastern North Pacific basins. Wea. Forecast. 14:326–37.

- 326 DeMaria, M., M. Mainelli, L.K. Shay, J.A. Knaff and J. Kaplan. 2005. Further improvements to
327 the Statistical Hurricane Intensity Prediction Scheme (SHIPS). *Wea. Forecast.* 20:531–
328 43.
- 329 DeMaria, M., J.A. Knaff and J. Kaplan. 2006. On the decay of tropical cyclone winds crossing
330 narrow landmasses. *J. Appl. Meteor. Climatol.* 45:491–99.
- 331 Evans, A.D. and R.J. Falvey. 2013. Annual Joint Typhoon Warning Center tropical cyclone
332 report. <http://www.usno.navy.mil/NOOC/nmfc-ph/RSS/jtwc/atcr/2012atcr.pdf>.
- 333 Franklin, J.L. cited 2010: 2009 National Hurricane Center verification report. [Available online
334 at http://www.nhc.noaa.gov/verification/pdfs/Verification_2009.pdf.]
- 335 Gall, R., J. Franklin, F. Marks, E.N. Rappaport and F. Toepfer. 2013. The Hurricane Forecast
336 Improvement Project. *Bull. Amer. Meteor. Soc.* 94:329-43.
- 337 Goldenberg, S.B., S.G. Gopalakrishnan, X. Zhang, V. Tallapragada, S. Trahan, T. Quirino, F.
338 Marks and R. Atlas. 2015. The 2012 triply-nested, high-resolution operational version of
339 the Hurricane Weather Research and Forecasting System (HWRF): Track and intensity
340 forecast verifications. *Wea. Forecast.* 30(3):710-29.
- 341 Gopalakrishnan, S.G., F. Marks, X. Zhang, J.-W. Bao, K.-S. Yeh and R. Atlas. 2011. The
342 experimental HWRF System: A study on the influence of horizontal resolution on the
343 structure and intensity changes in tropical cyclones using an idealized framework. *Mon.*
344 *Wea. Rev.* 139:1762-84.
- 345 Gopalakrishnan, S.G., S. Goldenberg, T. Quirino, F. Marks, X. Zhang, K.-S. Yeh, R. Atlas and
346 V. Tallapragada. 2012. Towards improving high-resolution numerical hurricane
347 forecasting: Influence of model horizontal grid resolution, initialization, and physics.
348 *Wea. Forecast.* 27(3):647-66. doi:10.1175/WAF-D-11-00055.1 2012.

- 349 Gopalakrishnan, S.G., F. Marks, J.A. Zhang, X. Zhang, J.-W. Bao and V. Tallapragada. 2013. A
350 study of the impacts of vertical diffusion on the structure and intensity of the tropical
351 cyclone using the high-resolution HWRF system. *J. Atmos. Sci.* 70:524-41.
- 352 Kieu, C.Q., V. Tallapragada and W. Hogsett. 2014. Vertical structure of tropical cyclones at
353 onset of the rapid intensification in the HWRF model. *Geophys. Res. Lett.* 41:3298-306.
- 354 Mohanty, U.C., K.K. Osuri, V. Tallapragada, F.D. Marks, S. Pattanayak, M. Mohapatra, S.G.
355 Gopalakrishnan and D. Niyogi. 2015. A Great escape from the Bay of Bengal “Super
356 Sapphire-Phailin” tropical cyclone - A case of improved weather forecast and societal
357 response for disaster mitigation. *Earth Interact.* Accepted for publication.
- 358 Rappaport, E.N. and Coauthors. 2009. Advances and challenges at the National Hurricane
359 Center. *Wea. Forecast.* 24:395–419.
- 360 Tallapragada, V., C. Kieu, Y. Kwon, S. Trahan, Q. Liu, Z. Zhang and I. Kwon. 2013. Evaluation
361 of storm structure from the operational HWRF model during 2012 implementation. *Mon*
362 *Wea. Rev.* 142(11):4308-25. <http://dx.doi.org/10.1175/MWR-D-13-00010.1>.
- 363 Tallapragada, V. and C. Kieu. 2014a. Real-time forecasts of typhoon rapid intensification in the
364 north western Pacific Basin with the NCEP operational HWRF model. *Trop. Cycl. Res.*
365 *Rev.* 3(2):63-77.
- 366 Tallapragada, V., L. Bernardet, S. Gopalakrishnan, Y. Kwon, Q. Liu, T. Marchok, D. Sheinin,
367 M. Tong, S. Trahan, R. Tuleya, R. Yablonsky and X. Zhang. 2014b. Hurricane Weather
368 and Research and Forecasting (HWRF) model: 2014 scientific documentation, 99 pp.
369 (http://www.dtcenter.org/HurrWRF/users/docs/scientific_documents/HWRFv3.6a_ScientificDoc.pdf).
- 370

- 371 Tallapragada, V., C. Kieu, S. Trahan, Z. Zhang, Q. Liu, W. Wang, M. Tong, B. Zhang and B.
372 Strahl. 2015a. Forecasting tropical cyclones in the western North Pacific Basin using the
373 NCEP operational HWRF model. Real-time implementation in 2012. *Wea. Forecast.*
374 <http://dx.doi.org/10.1175/WAF-D-14-00138.1>.
- 375 Tallapragada, V., C. Kieu, S. Trahan, Q. Liu, W. Wang, Z. Zhang, M. Tong, B. Zhang, L.-L. Zhu
376 and B. Strahl. 2015b. Forecasting tropical cyclones in the western North Pacific Basin
377 using the NCEP operational HWRF model. Model upgrades and evaluation of real-time
378 performance in 2013. *Wea. Forecast.* Submitted.
379 http://www.emc.ncep.noaa.gov/gc_wmb/vxt/pubs/hwrf_wpac_part2.pdf.
- 380 Zhang, X., T. Quirino, K.-S. Yeh, S. Gopalakrishnan, F. Marks, S. Goldenberg and S. Aberson.
381 2011. HWRFx: Improving hurricane forecasts with high-resolution modeling. *Comp. Sci.*
382 *Eng.* 13:13-21.

383 Figure Captions

384 Figure 1. HWRF/GFDL model domains for providing real-time TC forecasts in different
385 ocean basins. Solid lines represent operational HWRF domains coupled to the
386 MPIPOM ocean model. Dashed lines show uncoupled model forecasts provided by
387 HWRF in real time.

388 Figure 2. Average intensity forecast errors in knots for the Atlantic Basin during the 2010-
389 2012 hurricane seasons based on the 2013 version of the HWRF model (H3FI;
390 27:9:3 km) compared to the 2012 version (H2FI; 27:9:3 km), the original
391 operational HWRF model (HWFI; 27:9 km), the GFDL model (GHMI), and
392 statistical models LGEM (Linear Growth Equation Model) and DSHP (Decay
393 Statistical Hurricane Intensity Prediction System). Black line represents NHC's
394 official forecast errors as a function of time, and the number of cases verified at
395 each forecast period is shown along the x-axis.

396 Figure 3. Forecast improvements in the NATL basin from the operational HWRF model since
397 2011. Each configuration of HWRF was evaluated for multiple hurricane seasons.
398 The dashed lines shows the HFIP baseline (BASE) and 5-year goal for track and
399 intensity errors. The samples are non-homogeneous, and the number of cases
400 verified at the initial time for each configuration is provided in parentheses. HWRF
401 (in purple) represents operational forecasts during 2007-2011 prior to the
402 implementation of the high-resolution version in 2012. H212, H213, H214, and
403 H215 represent, respectively, the 2012, 2013, 2014, and 2015 HWRF versions.

404 Figure 4. Top: Non-homogenous comparison of the absolute track forecast errors between the
405 2012 HWRF version during 2012 (blue columns) and the 2013 HWRF version

406 during 2013 (red columns). Bottom: similar to (a) but for the absolute intensity
407 forecast errors.

408 Figure 5. Verification of the absolute track errors (top) and absolute intensity errors (bottom)
409 during 2013 for typhoons in the WPAC basin for HWRF (red), COAMPS-TC
410 (blue), AVNO (GFS) (black), GFDN (cyan), and JTWC's official forecast (purple).
411 The numbers below the x-axis denote the number of cases verified for each forecast
412 time.

413 Figure 6. HWRF forecast of the life cycle of TC Phailin starting from (a) genesis at 06 UTC 6
414 Oct 2013, (b) formation of depression on 8 Oct 2013, (c) intensification, and (d)
415 dissipation. Shading depicts the microwave satellite imagery (37 GHz) equivalent
416 from the model, and contours represent minimum sea level pressure (hPa). The
417 black line represents the best track from JTWC, and the white line is the HWRF
418 predicted track from 00 UTC 10 October 2013.

419 Figure 7. Verification of the average absolute track errors (top) and average absolute intensity
420 errors (bottom) during 2013 for tropical cyclones in the NIO for HWRF (red),
421 COAMPS-TC (COTC, blue), AVNO (GFS, black), GFDN (cyan), and JTWC's
422 official forecast (purple). The numbers below the x-axis denote the number of cases
423 verified for each forecast time.

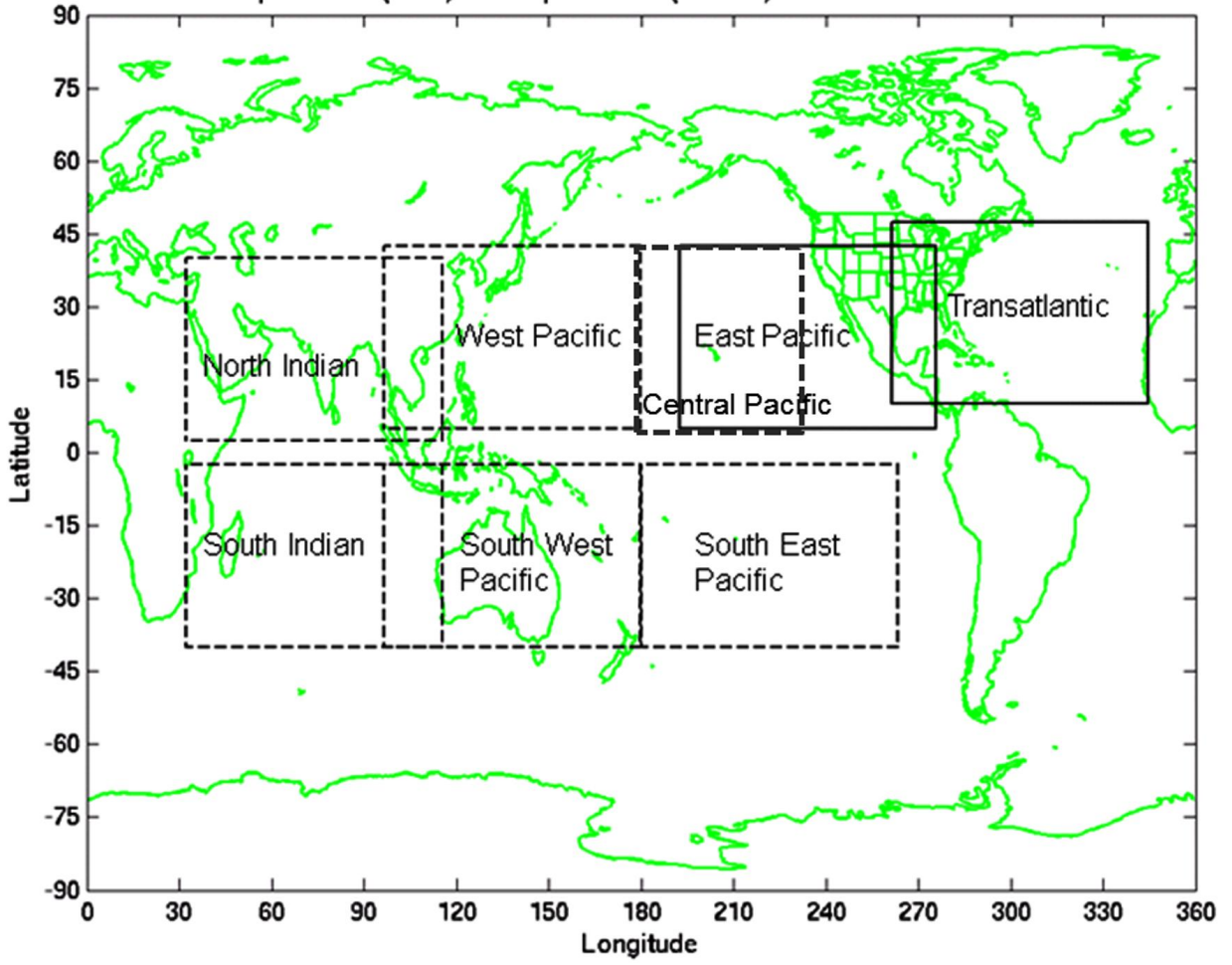
424 Figure 8. (a) Radius-height, azimuthally-averaged cross section of the relative humidity
425 (shaded, unit percent), tangential wind (black contours at intervals of 3 m s^{-1}), and
426 potential temperature anomalies with respect to the far-field environment (red
427 contours at intervals of 10 K, solid/dotted contours for positive/negative values) in
428 an idealized experiment with the HWRF model compared to an analysis of storm

429 vertical structure at the time of RI onset for (b) 6-h forecast of STY Soulik and (c)
430 18-h forecast of STY Usagi.

431 Figure 9. Scatter plots of the 24-h change of the maximum 10-m winds (in m s^{-1}) from
432 observations (BEST, x-axis) and real-time model forecasts (HWRF, y-axis) for
433 2013 (left panel) and 2012 (right panel). Black boxes denote the points that both
434 HWRF and the observations capture RI, whereas gray boxes denote the points that
435 HWRF forecasts RI events that were not observed in reality.

436 Figure 10. Basin scale HWRF model with multiple moving nests covering the Atlantic and
437 East Pacific basins valid at 18 UTC 26 Aug 2010. Shading represents sea level
438 pressure, and the steering flow is represented by wind vectors over the static
439 domain set at 27-km resolution. In this case, the nest at 3-km resolution covers TCs
440 Danielle and Earl in the Atlantic and Frank in the East Pacific. Brightness
441 temperatures are shown in the high resolution nest. Inset: Basin scale HWRF
442 (green) and observed (blue) evolution of 10-m-wind speeds for Earl (top left),
443 Danielle (top right), and Frank (bottom). Please refer to
444 http://hwrf.aoml.noaa.gov/pix/website/HWRF-Basinscale_06L-07L-09E.gif for the
445 animation.

446

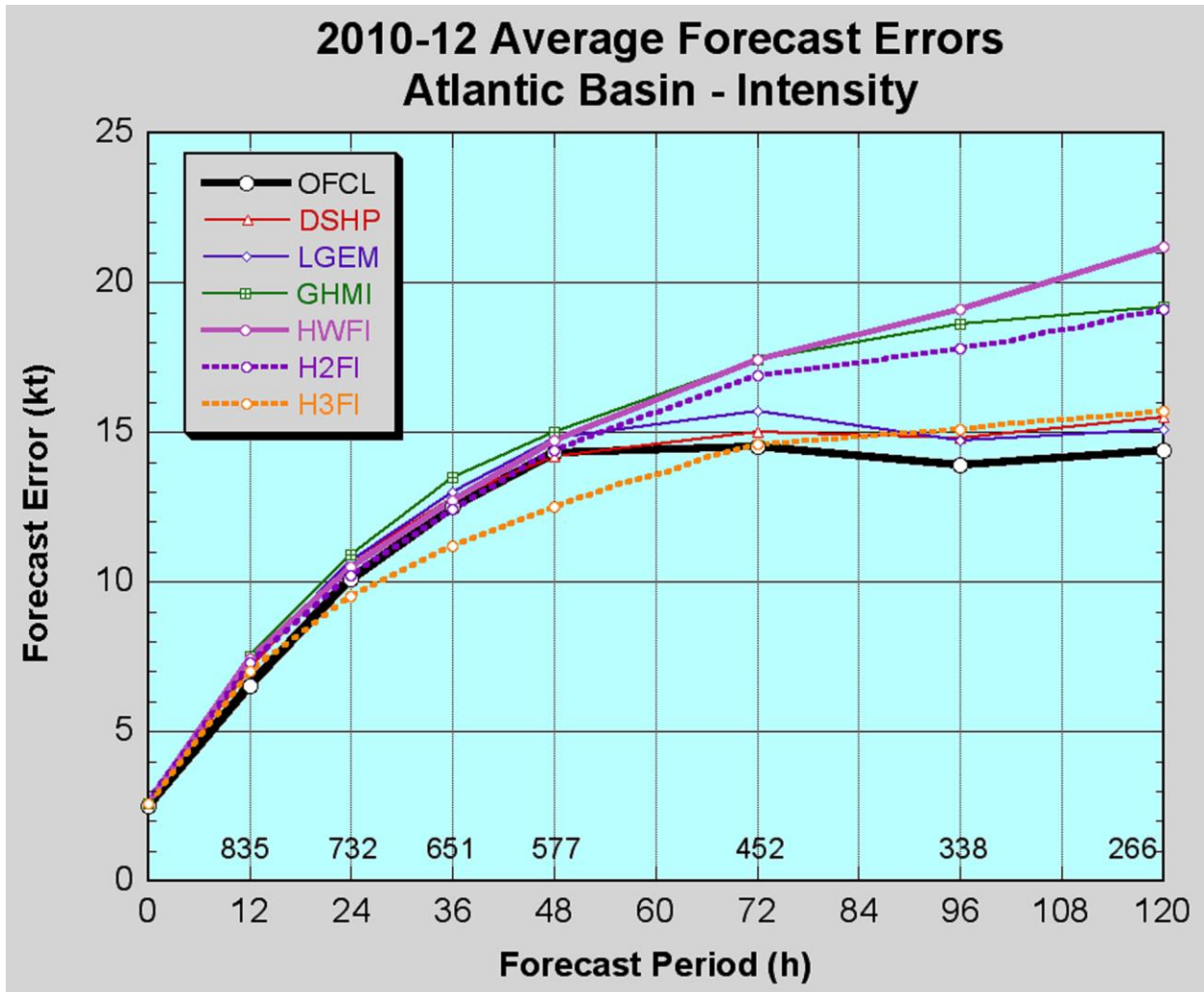


447

448

449

Figure 1

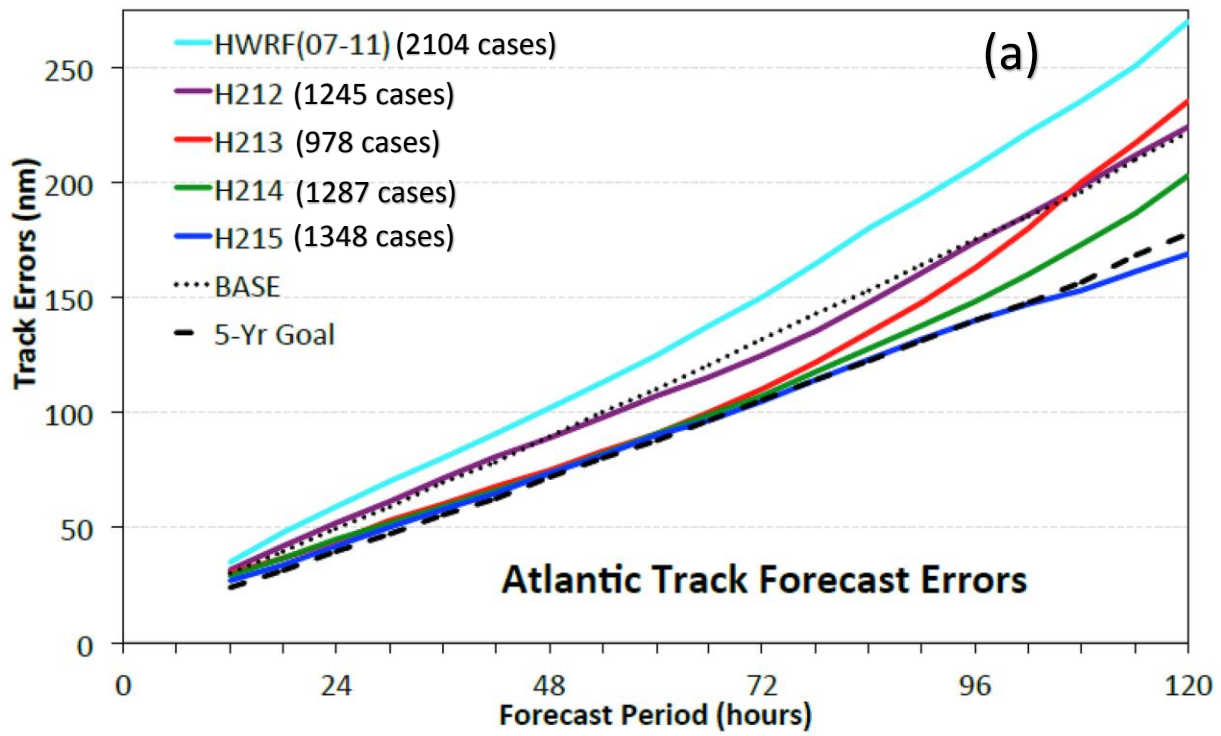


450

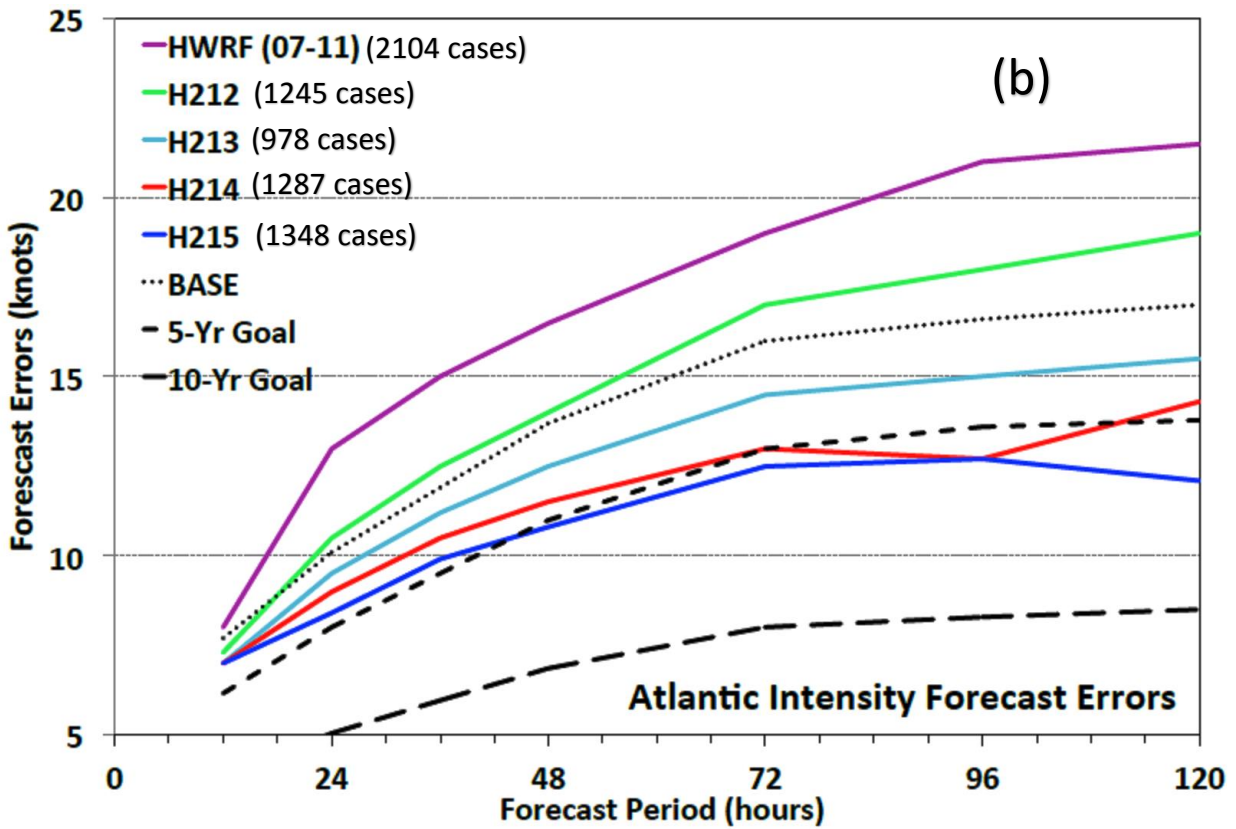
451

452

Figure 2



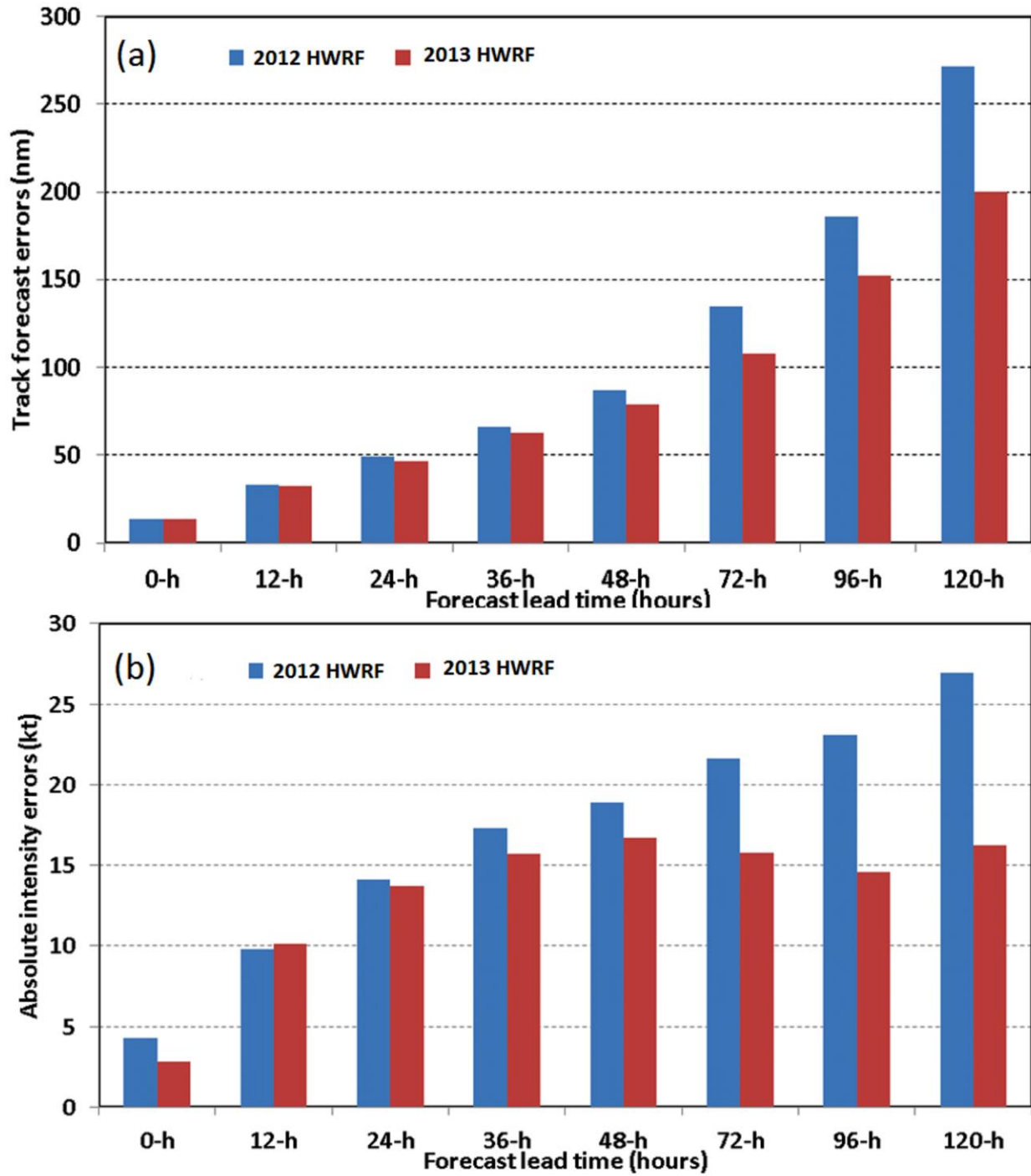
453



454

455

Figure 3

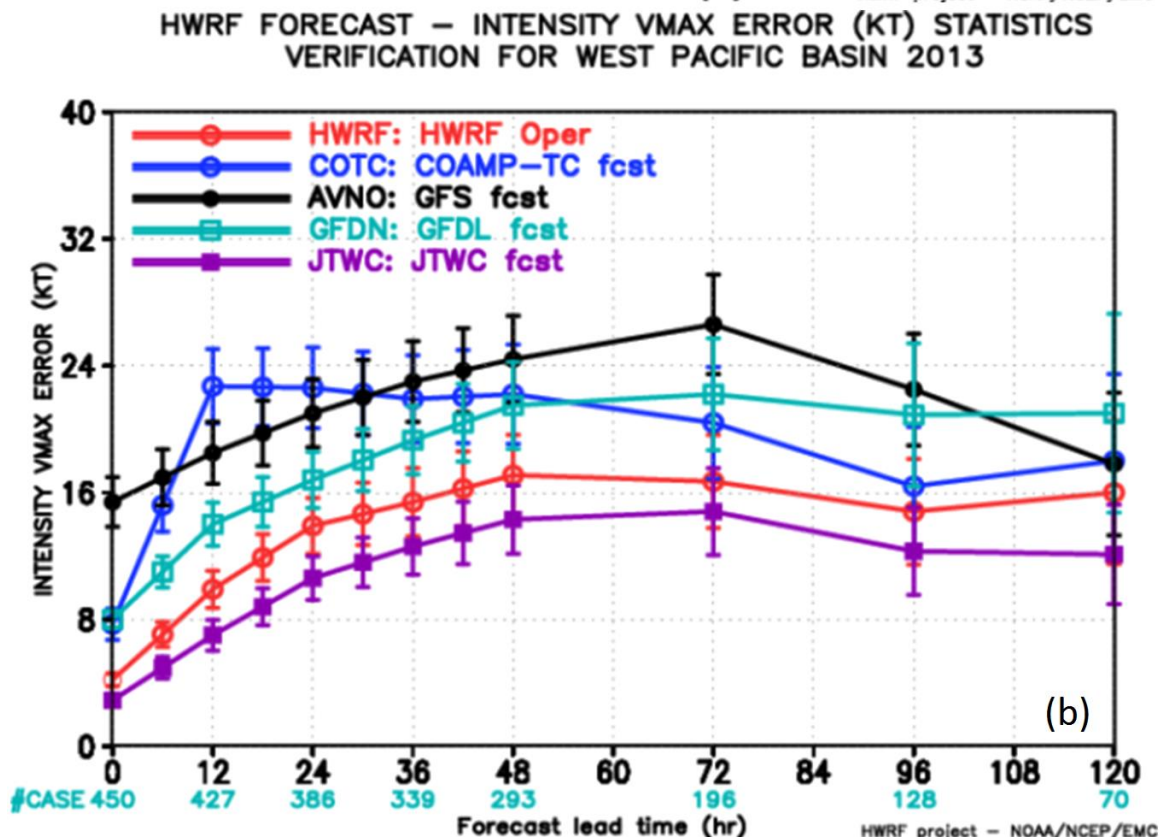
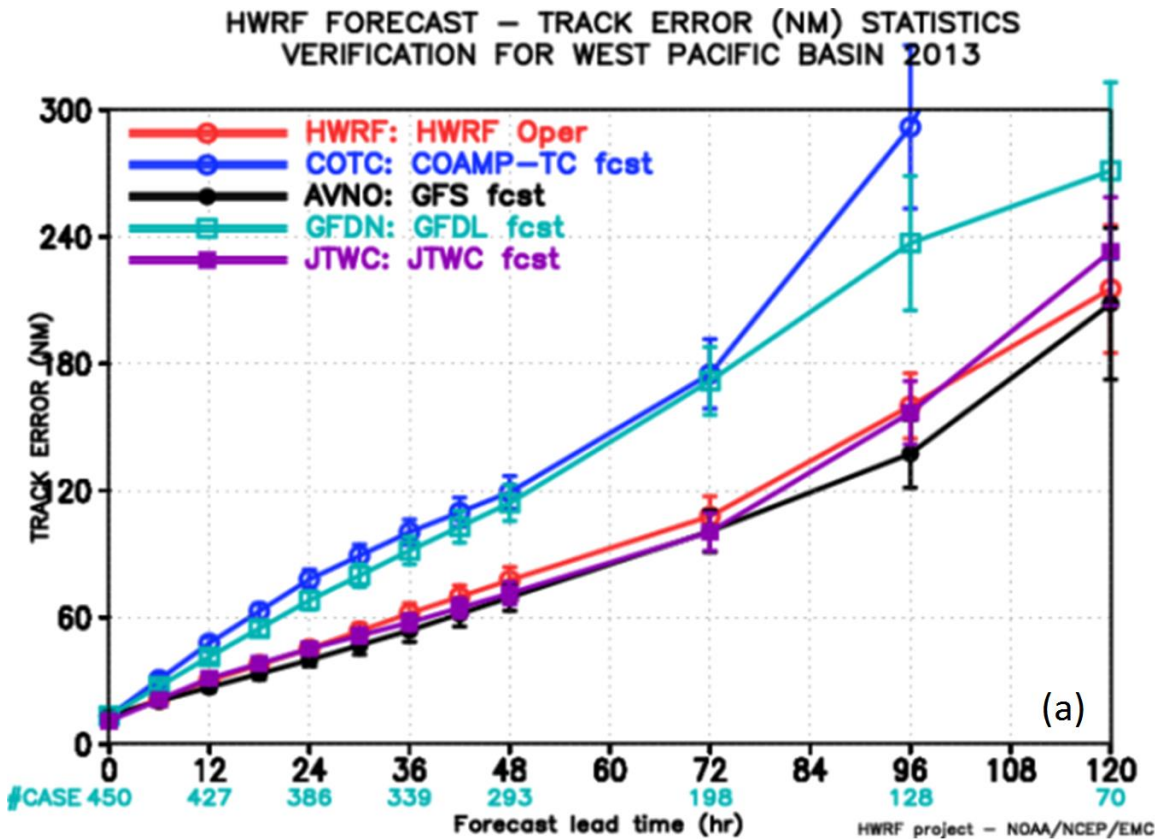


456

457

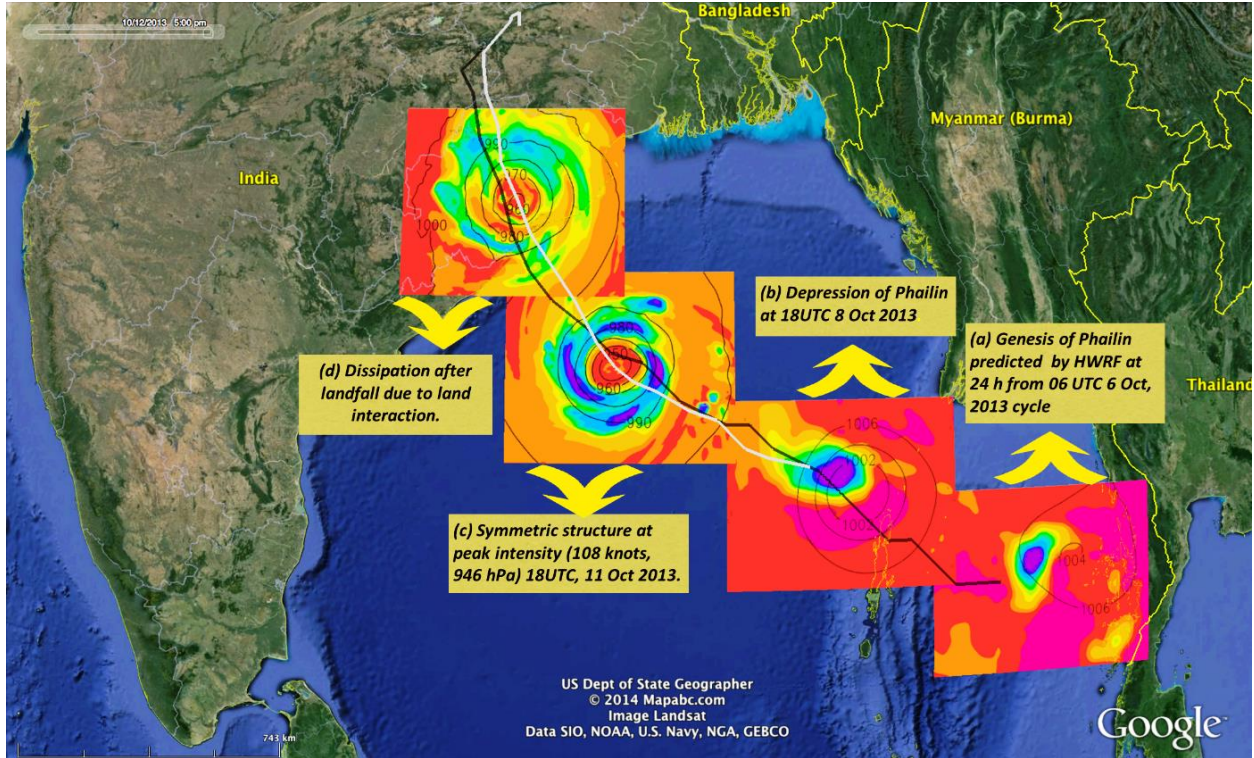
458

Figure 4



459
460

Figure 5

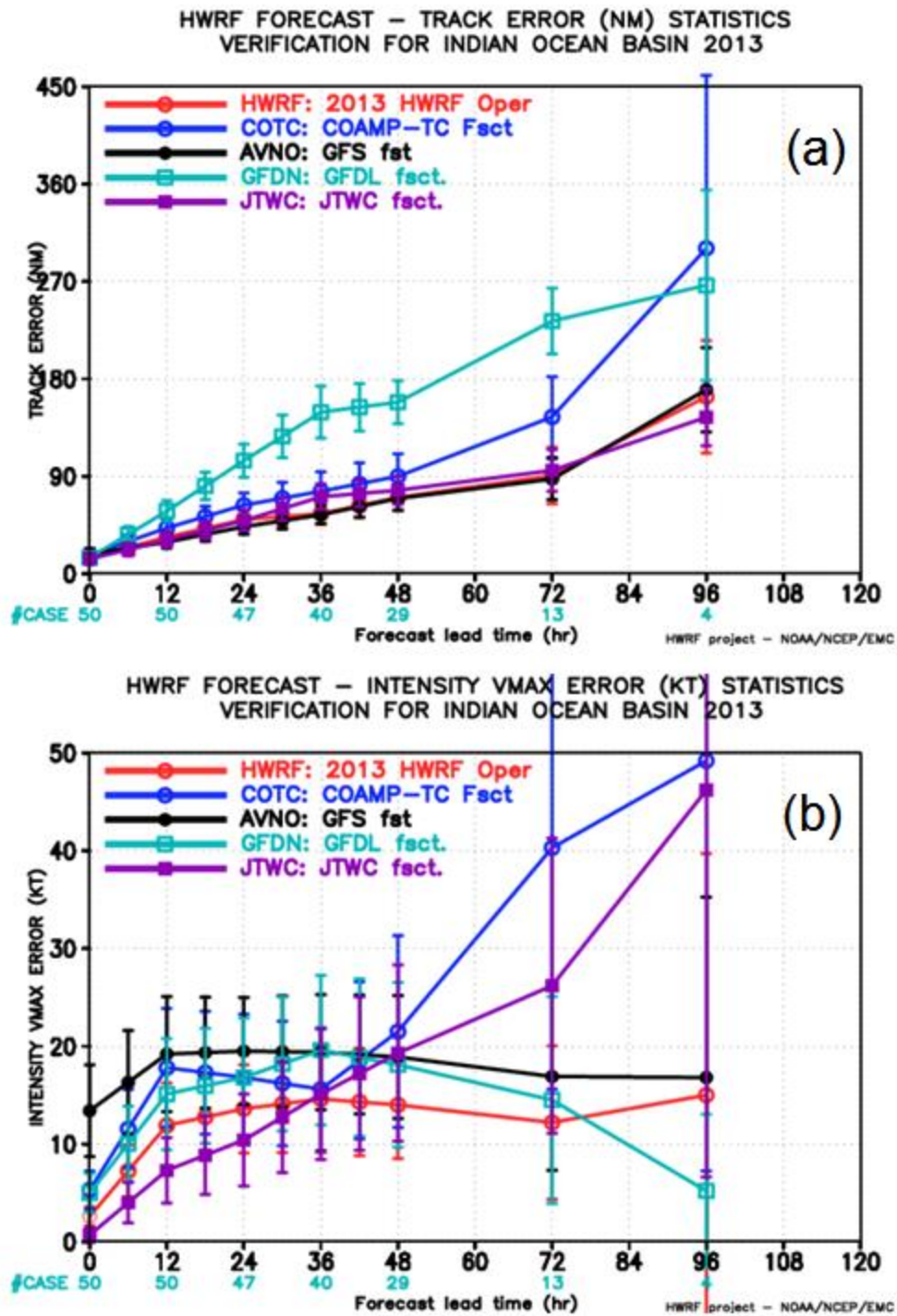


461

462

463

Figure 6

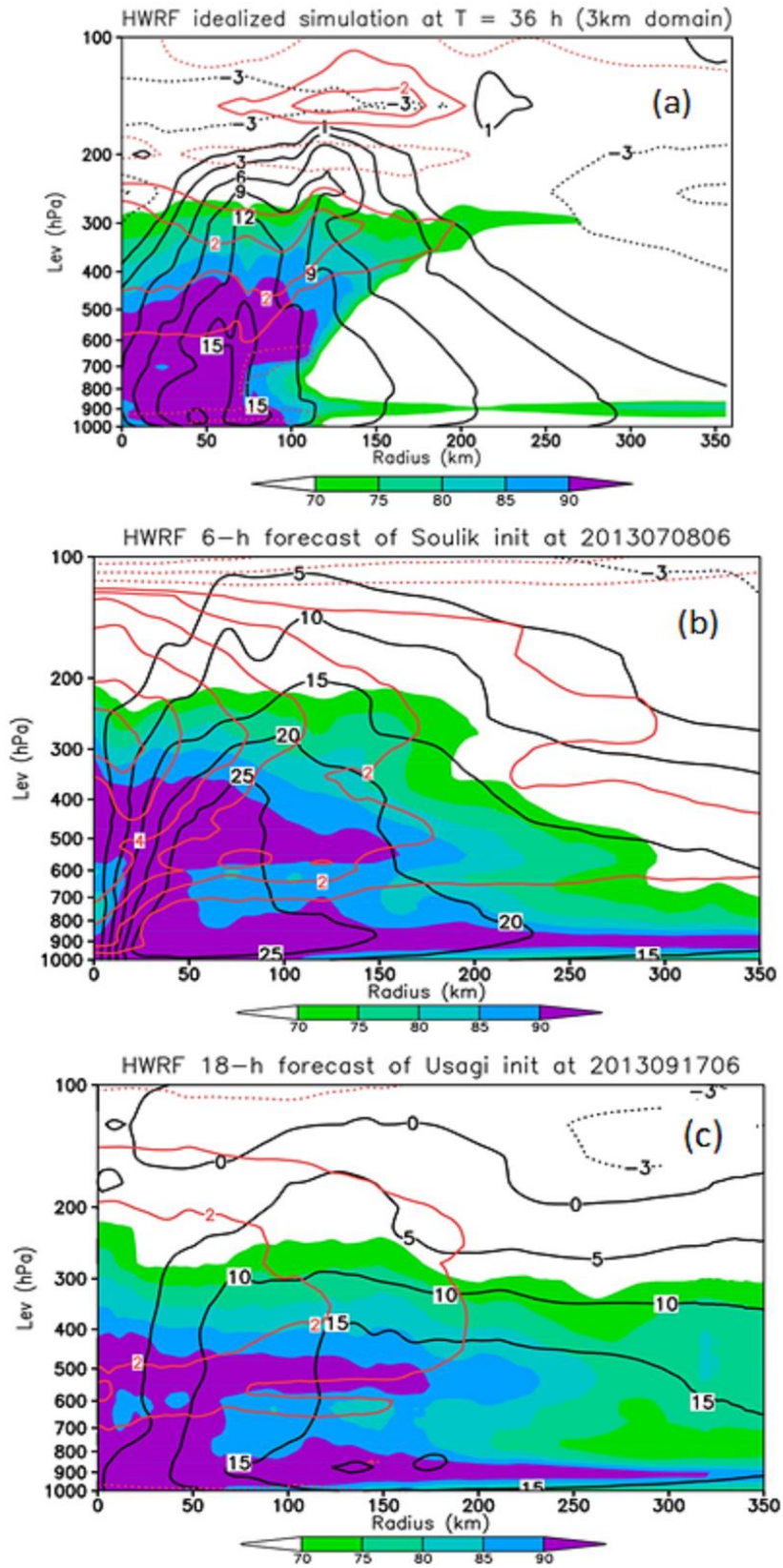


464

465

466

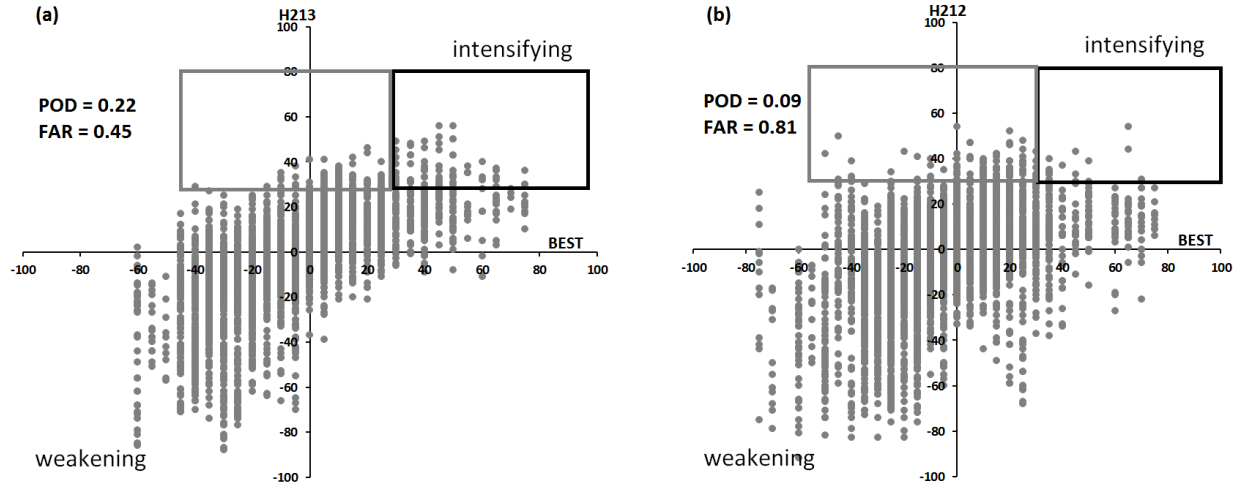
Figure 7



467

468

Figure 8

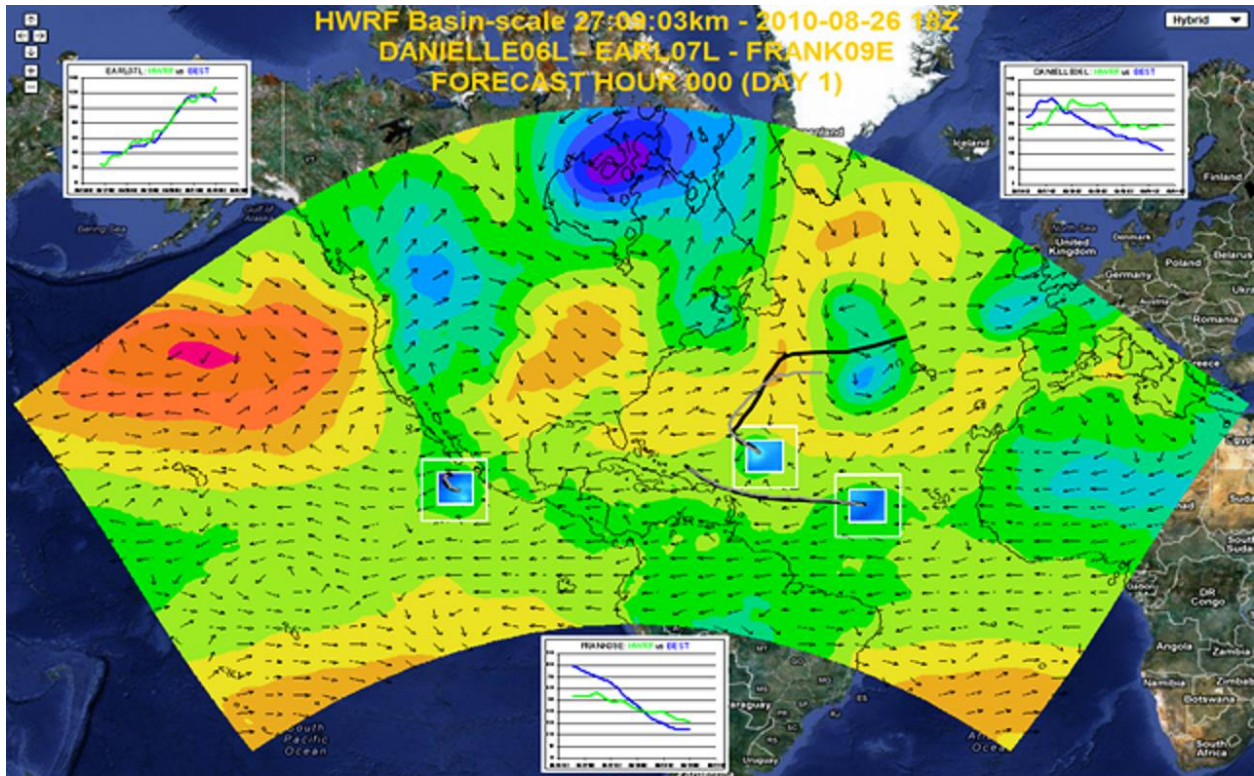


469

470

471

Figure 9



472

473

Figure 10